Dose-Response:
An International Journal
July-September 2018:1-8

DOI: 10.1177/1559325818789841
journals.sagepub.com/home/dos
SAGE

The Effect of Photothermal Therapy on Osteosarcoma With Polyacrylic Acid–Coated Gold Nanorods

Su Pan[1,*], Hongcun Xing[2,*], Xuqi Fu[2], Hongmei Yu[3], Zhaogang Yang[4], Yudan Yang[3], and Wei Sun[5]

Abstract

Background: Polyacrylic acid (PAA)–coated gold nanorods (GNRs) were prepared in this research, and then the structure, stability, temperature increment efficiency, and biocompatibility of GNRs@PAA were detected.

Methods: It was demonstrated that GNRs@PAA coupled with an 808 nm laser had superior efficiency of hyperthermia therapy for MG63 human osteosarcoma cell.

Results: The mechanism of photothermal therapy of GNRs@PAA was explored, and it was proved that damaged cell membrane and DNA integration caused cell apoptosis and death, and the cell apoptosis rate had been obviously promoted by in vitro photothermal therapy which exhibited time–dose dependence.

Conclusion: The results demonstrated that the GNRs@PAA could be a promising candidate for phototherapeutic applications in human osteosarcoma.

Keywords

osteosarcoma, photothermal therapy, metal nanostructures, apoptosis, time–dose dependent

Introduction

Osteosarcoma is the most typical tumor in primary malignant tumor of bone and soft tissue which has a high incidence rate, a high degree of malignancy, and an early metastasis. At present, surgical treatment, radiotherapy, and high-dose chemotherapy are the main treatments for osteosarcoma. In the past decades, these therapeutic methods have been greatly improved, but the effect is unsatisfactory; for a 5-year survival rate, the effect still does not exceed 60%, and it is accompanied by more serious side effects including drug tolerance and secondary tumors caused by chemotherapy.[1] Therefore, it is essential to explore new methods and approaches for the treatment of osteosarcoma.

Photothermal therapy of tumors is a mild, high-performance, and noninvasive method developed in recent years. In the case of light irradiation, the morphology and function of normal cells can be ensured based on killing the tumor cells. Therefore, photothermal therapy has better selectivity and fewer side effects which can combine with the traditional treatment method, so it has caused more and more attention in the treatment of bone and soft tissue tumors.

With the development of nanotechnology, various nanoparticles (NPs) have been used in the diagnosis and treatment of tumors.[2-6] At present, for the predominant surface plasmon

[1] Department of Orthopedics, The Second Hospital of Jilin University, Changchun, Jilin, China
[2] College of Life Sciences, Jilin University, Changchun, Jilin, China
[3] China-Japan Union Hospital of Jilin University, Changchun, Jilin, China
[4] Department of Chemical and Biomolecular Engineering, The Ohio State University, Columbus, OH, USA
[5] Department of Molecular Biology, College of Basic Medical Sciences, Jilin University, Changchun, Jilin, China
* These authors contributed equally to this study.

Received 23 June 2018; received revised 20 June 2018; accepted 26 June 2018

Corresponding Authors:
Wei Sun, College of Basic Medical Sciences, Jilin University, 126 Xinmin Street, Changchun, Jilin 130021, China.
Email: s_wei@jlu.edu.cn

Yudan Yang, China-Japan Union Hospital of Jilin University, Changchun, Jilin 130021, China.
Email: yangyudan@jlu.edu.cn

resonance (SPR) absorption and scatter[7-10] of gold NPs, such as gold nanoshells, nanorod, and nanocages, gold NPs have proved to be used potentially in biomedical science, including drug loading, cell-targeted vectors, biosensor techniques, and photothermal tumor ablation.[11-16] In these gold NPs, GNRs are shown to be more towardly utilized than solid spherical NPs in biology and medicine including near-infrared region (NIR) laser photothermal therapy of tumor and targeted drug delivery. Gold nanorods (GNRs) display superior tunability in SPR absorbing through altering the length–breadth ratio and show pretty function in transforming light of NIR to heat energy; furthermore, light in NIR has maximum penetrating depth into human tissues.[17-21]

In this study, a PAA-coated GNR was prepared which has superior biocompatibility and good stiffness to observe the killing effect of it in the treatment of human osteosarcoma cell-line MG-63 in vitro and to investigate the preliminary mechanism of cell death, by which to provide new therapeutic approaches for clinical treatment of osteosarcoma.

Materials and Methods

Materials

$HAuCl_4 \bullet 3H_2O$ (99.99%), $AgNO_3$ (99.8%), polyacrylic acid (PAA, Molecular weight-15 000 g/mol and MW-45 0000 g/mol), $NaBH_4$ (98%), cetyltrimethylammonium bromide (99%), and ascorbic acid (99%) which were analytical reagents were purchased from Alfa Aesar (USA). Propidium iodide (PI) and Tris (99.0%) was bought from Sigma (USA). Analytical grade reagents such as NaOH, HCl, hydroquinol (98%), and sodium citrate (99.0%) were used immediately. Annexin V-FITC (Fluorescein isothiocyanate) Apoptosis Detection Kit (Vazyme Biotech Co, Ltd. China). Cell Counting Kit-8 (CCK-8; Dojindo, China), fetal bovine serum (FBS), trypsin, phosphate buffered saline (PBS), and dulbecco-modified eagle medium with high glucose (H-DMEM 12430-054) were purchased from Gibco (USA). Ultrapure water was used in all reagent and material dispensing. Human osteosarcoma cell line (MG63) was purchased from Shanghai Institute for Biological sciences, Chinese Academy of Science.

Preparation of GNRs@PAA

Gold nanorods were prepared according to the seed-mediated growth method by El-Sayed and coworkers. Briefly, a seed solution was prepared by mixing 7.5 mL of CTAB (hexadecyl trimethyl ammonium bromide) (0.1 mol/L) and 2.5 mL of HAuCl4 (1 mmol/L) with 0.6 mL freshly prepared 10 mmol/L NaHB4 solution under vigorous stirring at 28°C. After 2 hours, this seed solution was used for the synthesis of the GNRs. In a flask, 13.2 mL of 0.1 mol/L CTAB was mixed with 12 mL of 1 mmo/L $HAuCl_4$, then 240μL of 10 mmol/L silver nitrate aqueous solution, and 220 μL of 2 mol/L hydrochloric acid were added to the flask. After gently mixing the solution, 192 μL of 0.1 mol/L ascorbic acid was added. On continuously stirring this mixture, various concentrations of seed solution were added finally to initiate the growth of the GNRs. These nanorods were aged for 5 hours to ensure full growth at 28°C. After preparation, excess CTAB was removed by centrifuging twice at 12 000 rpm for 10 minutes and then redispersed in deionization water.[15]

Polyacrylic acid–coated GNRs were prepared by the versatile layer-by-layer approach. In brief, 2 mg/mL PAA-450 000g/moL was prepared in a 10 mmol/L NaCl solution (which was sonicated previously for 30 minutes). Then, 2 mL GNRs (2×) were added drop wise to the PAA solution (v/v = 1:1), and the mixture was stirred vigorously for 6 hours. The PAA-coated GNRs were separated by centrifugation 3 times to remove excess polyelectrolyte and then redispersed in 2 mL of PBS (pH 7.4). The PAA-15000g/moL–coated GNRs were prepared according to the method by Michael D. Wyatt.[22]

Nanoparticles Characterization

A Ultraviolet (UV)-1800 UV-vis-NIR spectrophotometer (Shimadzu, Japan) was used to detect the spectra of UV visible absorption of all samples for GNRs@PAA preparation ranging from 400 nm to 1100 nm wavelength in common experimental environment with room temperature. Transmission electron microscopy (TEM) images of PAA-coated GNRs were implemented by a Hitachi H-800 electron microscope (Japan) under 200 kV accelerating voltage with a charge coupled device camera. Fourier transform infrared (FTIR) spectra were measured using an IR Affinity-1 spectrophotometer (Avatar, Nicolet, USA). Bright-field and fluorescent mappings of MG63 cells were obtained using an Olympus IX51 inverted fluorescence microscope (Olympus, Japan).

Cell Culture

MG63 human osteosarcoma cells were cultured in H-DMEM and supplemented with 10% FBS and 1% penicillin–streptomycin. Cells were cultivated with humidified atmosphere of 5% CO_2 at 37°C which were split using trypsin medium when cell had grown to approximate 80% confluent in 6-well culture plate.

Cytotoxicity Assay

Colorimetric assay is one of the popular methods for quantifying the percentage of survival cells. The cytotoxicity of GNRs@PAA on MG63 cells were analyzed using the CCK-8 assay in this experiment. Briefly, MG63 cells (5×10^5 cells/mL density) were planted into 96-well plates with 100 μL H-DMEM medium and cultured for 24 hours with humidified atmosphere of 5% CO_2 at 37°C. Furthermore, the MG63 cells were incubated for 24 hours with GNRs@PAA conjugates with different concentrations (20 μg/mL, 40 μg/mL, 80 μg/mL, 120 μg/mL, and 160 μg/mL), and the MG63 cells in the control group were incubated in H-DMEM medium. Then, MG63 cells in all groups were treated with H-DMEM medium including 10% CCK-8 reagent for 1 hour to 4 hours. Finally, the absorbance of CCK-8 was determined at absorption wavelength of

450 nm by a microplate reader. The detected cell viability was presented as a relative percentage to control.

Photothermal Therapy

The efficiency of photothermal therapy with GNRs was investigated by detecting mortality rate of MG63 cells after being irradiated with the continuous wave laser at 808 nm. MG63 cells (5×10^5 cells/mL density) were planted into 96-well plates with 100 μL H-DMEM medium and cultured for 24 hours with humidified atmosphere of 5% CO_2 at 37°C. Then, the MG63 cells were incubated for 24 hours with GNRs@PAA conjugates at 80 μg/mL density, and the cell viabilities were detected by CCK-8 assay after laser irradiation at 808 nm with the power density of 1.5 W/cm^2 for various times (0 minute, 2 minutes, 5 minutes, 10 minutes, and 15 minutes).

Apoptosis Staining

The images of apoptosis or dead cells after photothermal therapy with GNRs@PAA were recorded using a fluorescence microscope of Olympus (Japan). MG63 cells were cultured in monolayer into 6-well plates with the density of 1×10^5 cell in each well for 24 hours in H-DMEM. Then, GNRs@PAA with 60 μg/mL density were added to each well and coincubated in H-DMEM medium for 24 hours. Furthermore, the unbound GNRs in H-DMEM medium were removed followed by washing 3 times with PBS. And thenMG63 cells were exposed to 808 nm laser with the power density of 1.5 W/cm^2 for 2 minutes and 5 minutes separately. The Apoptosis Detection kit with Annexin V-FITC and PI were used to obtain the image of cell. All experiments were done in triplicate.

Apoptosis Detection by Flow Cytometry

MG63 cells were cultured into 6-well plates for 24 hours, and then GNRs@PAA were added to each well in different concentrations (0, 10, 20, 40, 60, and 80 μg/mL) in triplicate and coincubated in H-DMEM medium for 24 hours. Furthermore, the unbound GNRs in H-DMEM medium were removed followed by washing 3 times with PBS. Then, MG63 cells were exposed to 808-nm laser with the power density of 1.5 W/cm^2 for 2 minutes and 5 minutes separately. The apoptosis rate of MG63 cells were determined by flow cytometry (FCM) using the Annexin V-FITC apoptosis detection kit flowing the protocol.

Statistical Analysis

Group data were presented as mean $\pm$ standard error of the mean. Unpaired *t* test was used to compare between the groups. The means of multiple groups were compared by analysis of variance followed by Least Significant Difference post hoc test. Differences with a 2-tailed $P < .05$ were considered statistically significant.

Results

Preparation of GNRs Coated With PAA

Gold nanorods predominantly absorb NIR light because of SPR, and the NIR light can penetrate deeply into human tissues, so GNRs can be used in photothermal therapy of carcinoma in human body. To reduce the toxicity and increase the biocompatibility during photothermal therapy, GNRs were modified with PAA for photothermal ablation in human osteosarcoma cells. Figure 1A primitively illustrated the prepared procedure of GNRs@PAA and photothermal therapy for carcinoma.

Transmission Electron Microscopy Image and UV–vis Spectroscopy Test of GNRs@ PAA

In order to study the dispersity of GNRs@PAA in solution such as PBS, the TEM micrograph of the GNRs@PAA is shown in Figure 1B. The results showed that the GNRs@PAA was homogeneous and monodispersed, and the average aspect ratio of the GNRs were around 4.2 (length 44.3 nm and width 10.8 nm). Because the PAA polymer was a thin layer on GNRs, there were no obvious changes between the unmodified nanorods and GNRs@PAA.

The UV–vis spectroscopy test of GNRs@PAA is shown in Figure 1C. The results showed that there was a 3-nm red-shift in the plasmon band maximum caused by the coating of polymer layer. The 810 nm was for CTAB-GNRs, while the 813 nm was for the GNRs@PAA. There was no broadening of plasmon band in the UV–vis spectroscopy of GNRs@PAA.

Fourier Transform Infrared Spectra and Temperature Increment in GNRs@PAA

The FTIR measurements were used to determine the formation of PAA-modified GNRs which is shown in Figure 1D. The results showed that there was an apparent carboxyl band at -1710 cm^{-1} that proved the successful modification of PAA to GNRs by electrostatic interaction and demonstrated that there was apparently no influence on the position and intensity of NIR absorptions for GNRs.

The temperature increment in GNRs@PAA NPs solution was tested through different power density of NIR laser at 808 nm, and the results are shown in Figure 1E. The results showed that during the test process, by an 808 nm laser with a power density of 0.5, 1.0, 1.5, and 2.0 W/cm^2, respectively, to irradiate the NPs solution, the temperature increased with the power density and time of irradiation, and the highest temperature could reach 63°C. The result demonstrated that the prepared GNRs@PAA was suitable for further photothermal therapy through hyperthermia.

Cytotoxicity Assay of GNRs@PAA

The biosafety is a fundamental factor to estimate NPs before in vivo application, so the cytotoxicity of GNRs@PAA on

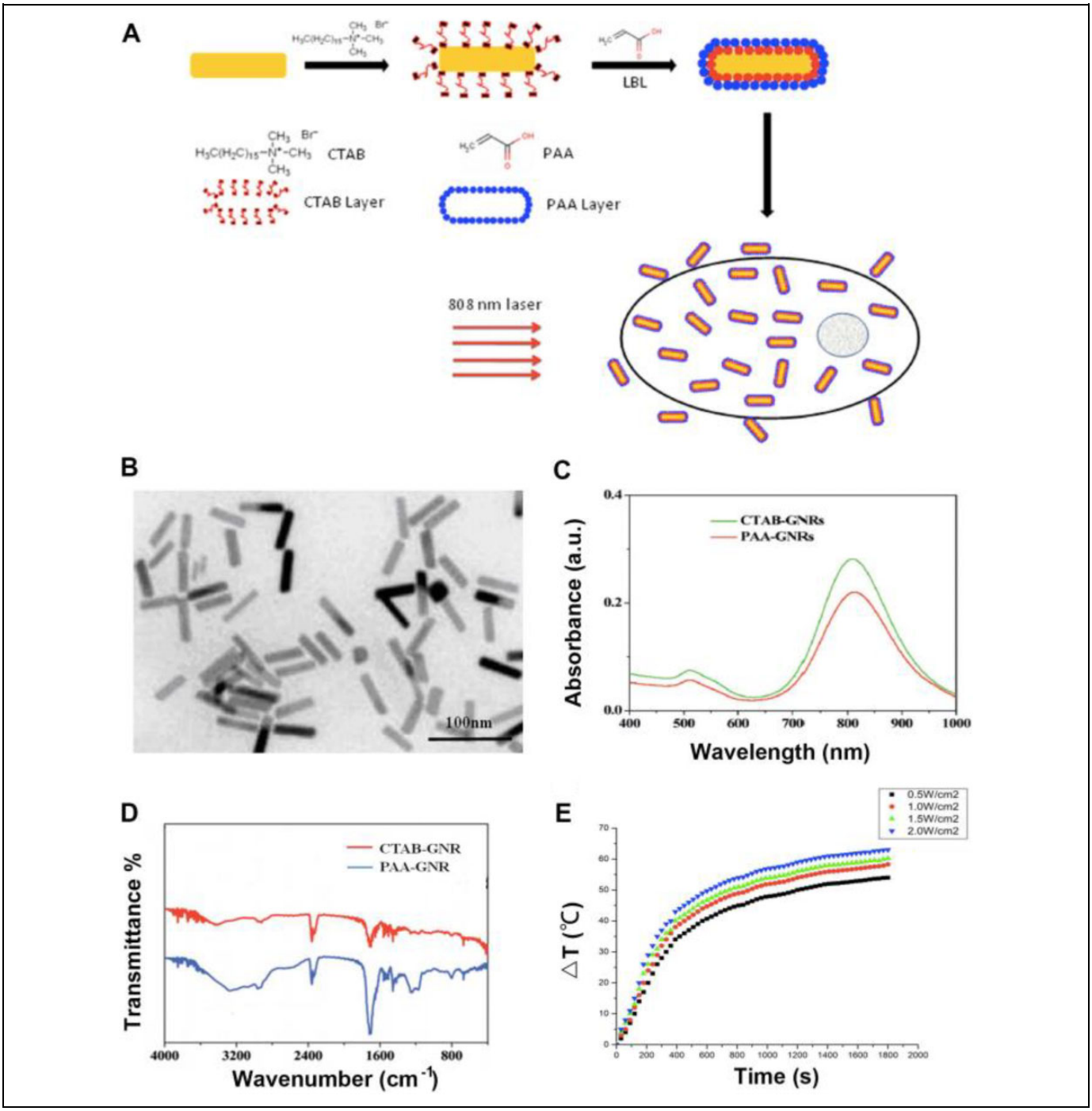

Figure 1. Scheme of GNRs@PAA photothermal therapy on cells and the characters of GNRs@PAA. A., Scheme indicating the process involved in the preparation of GNRs coated with PAA and photothermal therapy on cells. B., Transmission electron microscopy TEM image of GNRs@PAA. C., Absorption spectroscopy of GNRs@ PAA. D., Fourier transform infraredFTIR spectra of GNRs@PAA. E., The temperature increment of GNRs@PAA.

MG63 cell lines was detected by CCK-8 assay in this experiment (Figure 2A). Cells incubated with GNRs@PAA with different concentrations (20, 40, 80, 120, and 160 μg/mL) for 24 hours, and the results showed that the cell viability rates were all >80% in 20, 40, 80, and 120 μg/mL groups. It demonstrated that GNRs@PAA had superior biocompatibility.

Photothermal Ablation

To study the hyperthermia therapy efficiency of GNRs@PAA in vitro, MG63 cells were cultured with 80 μg/mL GNRs@PAA for 24 hours, and then, the culture medium including redundant GNRs@PAA was removed. Furthermore, cells were irradiated with laser power density of 1.5W/cm^2 for

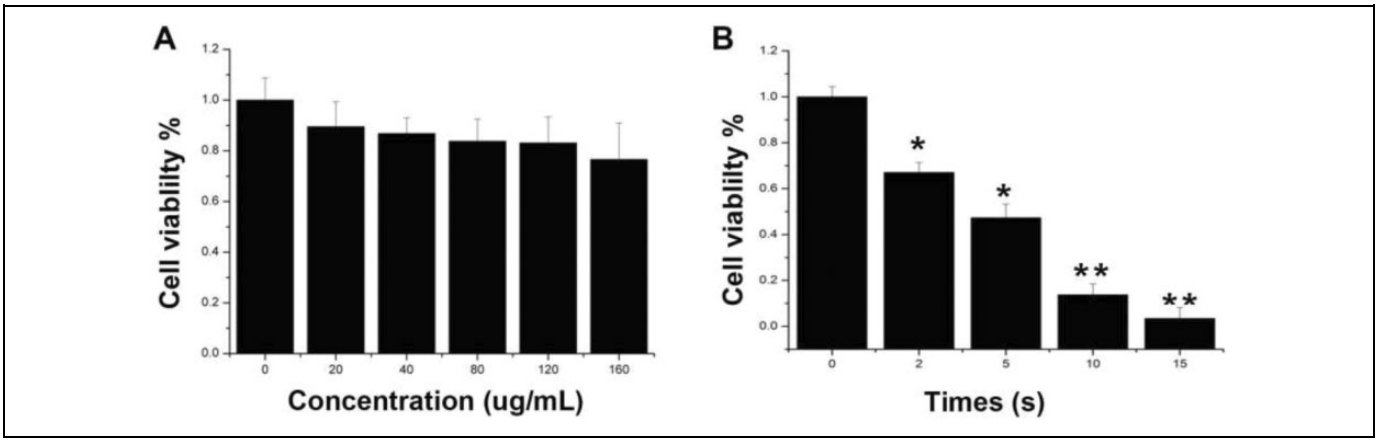

Figure 2. The cytotoxicity and photothermal therapies of GNRs@PAA in MG63 cells A, The cytotoxicity of GNRs@PAA in MG63 cells. B, Photothermal therapies of GNRs@PAA in MG63 Cells. MG63 cells are incubated with 80 μg/mL GNRs@PAA for 24 hours, and the cell viabilities were detected by CCK-8 assay after 808-nm laser irradiation with the power density of 1.5 W/cm^2 by different times. Data are shown as means ± standard error of the means, *$p < 0.05$ and **$p < 0.01$.

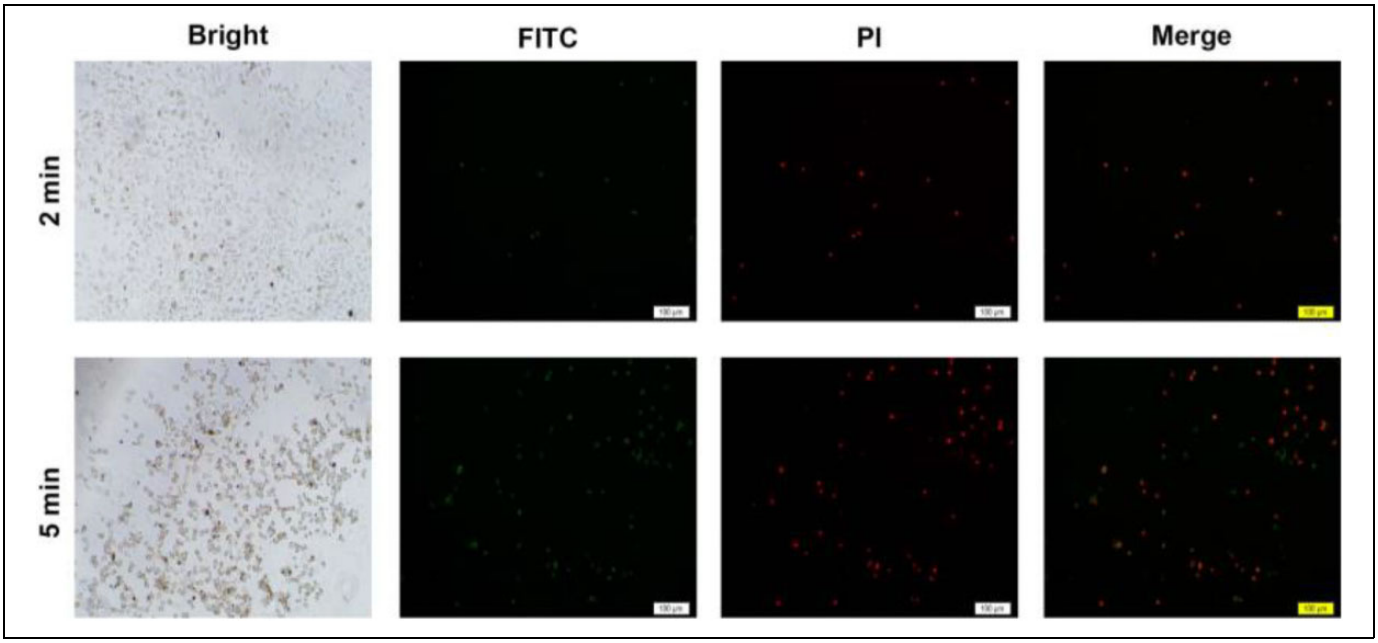

Figure 3. Apoptosis staining of MG63 cell. Fluorescent and bright field images of MG63 cells after photothermal therapies by an 808-nm laser with the power density of 1.5 W/cm^2 for 2 minutes and 5 minutes separately. The scale bar is 100 μm. Dose –response page 20 of 21.

different periods of 0, 10, 15, and 20 minutes, respectively, followed by CCK-8 assay (Figure 2B). The results demonstrated that the cell viabilities decreased with irradiation time, 55% of the MG63 cells were dead at 5 minutes, while 95% MG63 cells were dead at 15 minutes. It demonstrated that GNRs@PAA had superior efficiency of hyperthermia therapy for human osteosarcoma cell.

Apoptosis Staining

To study the hyperthermia therapy efficiency of GNRs@PAA in vitro, MG63 cells were cultured with GNRs@PAA for 24 hours, and then the unbound GNRs in the medium were removed. Furthermore, MG63 cells were exposed to 808-nm laser with the power density of 1.5 W/cm^2 for 2 minutes and 5 minutes separately followed by assay of apoptosis detection kit with Annexin V-FITC and PI as shown in Figure 3. The results demonstrated that there were only several apoptosis cells (representation as green as shown in Figure 3) and modicus necrotic cells (representation as red as shown in Figure 3) in the irradiation area with laser of 808 nm for 2 minutes, and it demonstrated that the GNRs@PAA only caused little injuries to the MG63 cells in this group. Furthermore, compared to the abovementioned group after irradiation with laser at 808 nm for 5 minutes, the "green" apoptosis cells and the "red" necrotic cells increased significantly, and the results demonstrated that

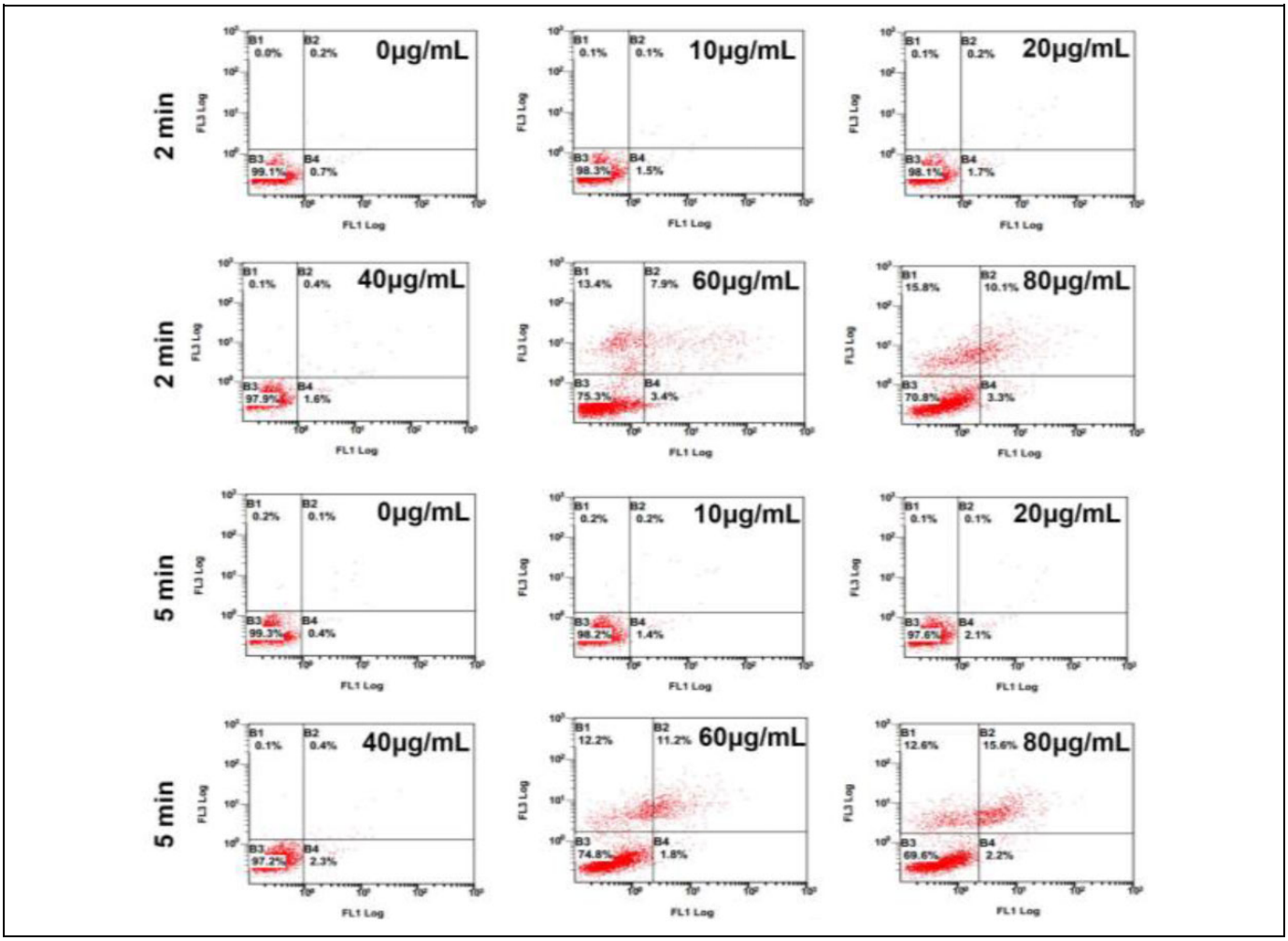

Figure 4. Flow cytometry of apoptosis MG63 cell Aafter Pphotothermal Ttherapies by an 808-nm laser with the power density of 1.5 W/cm^2 for 2 minutes and 5 minutes separately with GNRs@PAA at different concentration.

the efficiency of hyperthermia therapy by GNRs@PAA on MG63 cell increased with the elongation of irradiation time. Although it was proposed by some researchers that the death of carcinoma cell was caused by DNA damage when hyperthermia conditions got to 42°C to 43°C, the mechanism is still unclear up to now. The cell images in bright field of this experiment indicated that cells irradiated with laser of 808 nm showed plasmalemma disruption including bubble formation and thermic fragmentation. Furthermore, the cell image in dark imaging field showed DNA condensation which represented as high green or high red, and the results indicated that the cell death caused by GNRs@PAA was because of the damaged membrane of MG63 cell and the integrated DNA.

Quantification of Apoptosis Rate

MG63 cells incubated with GNRs@PAA with different concentration (0, 10, 20, 40, 60, and 80 μg/mL) for 24 hours and were exposed to 808-nm laser with the power density of 1.5 W/cm^2 for 2 minutes and 5 minutes separately, followed by apoptosis detection of FCM. The apoptotic rate was significantly increased by GNRs@PAA (0.11% ± 0.12%; 10 μg/mL; 0.23% ± 0.09%; 20 μg/mL; 0.46% ± 0.19%; 40 μg/mL; 8.12% ± 0.32%; 60 μg/mL; 12.02% ± 0.33%; 80 μg/mL; $P < .05$) in comparison to 0 μg/mL GNRs@PAA for 2 minutes. And the apoptotic rate was significantly increased by GNRs@PAA (0.21% ± 0.18%, 10 μg/mL; 0.18% ± 0.16%, 20 μg/mL; 0.51% ± 0.27%, 40 μg/mL; 10.62% ± 0.41%, 60 μg/mL; 15.34% ± 0.49%, 80 μg/mL; $P < .05$) compared to 0 μg/mL GNRs@PAA for 5 minutes. The results indicated that the apoptosis rate of MG63 cells had been promoted by in vitro photothermal therapy with GNRs@PAA at 60 and 80 μg/mL concentrations, and it exhibited time–dose dependence (Figure 4).

Discussion

Gold nanorods are potential candidates for the unique plasmonic properties which can be applied in the biomedical research such as delivery of gene,[23-27] imaging in biological, photothermal treatment of cancer,[28-32] and the biomolecular detection.[33-35] The main advantages of GNRs are their

remarkable absorption and scattering in the visible and NIR regions enhanced by SPR, fluorescence, biocompatibility, and tunable aspect ratio and ease of biofunctionalization. Gold nanorods have a relatively high near infrared absorption coefficient when compared to that of carbon nanotubes and are highly stable in comparison to silver nanoprisms.[32] Furthermore, the thermal conductivity of the surface layer in GNRs@PAA could be enhanced by encapsulation with PAA.[33]

Polyacrylic acid–coated GNRs were prepared in this experiment, and it was demonstrated that PAA was successfully modified to GNRs by electrostatic interaction, while there was no apparent influence on the position and intensity of NIR absorptions for GNRs. Furthermore, it was demonstrated that the GNRs@PAA are homogeneous and monodispersed, and the GNRs@PAA was not aggregated during modification with PAA. It demonstrated that GNRs@PAA had superior biocompatibility to MG63 human osteosarcoma cell which was suitable for further photothermal therapy through hyperthermia. The efficacy of in vitro photothermal therapy on MG63 cells by GNRs@PAA coupled with an 808-nm laser was investigated, and the result showed that GNRs@PAA had superior efficiency of hyperthermia therapy for human osteosarcoma cell. In addition, the mechanism of photothermal therapy of GNRs@PAA under laser irradiation was explored by apoptosis of staining and FCM detection and wound-healing assay. The results indicated that the cell death caused by GNRs@PAA was because of damaged-cell membrane and DNA integration, and the apoptosis rate of MG63 cells had been promoted by in vitro photothermal therapy which exhibited time–dose dependence, but it had no significant effect on migration of MG63 cell lines. The results demonstrated that the GNRs could be a promising candidate for phototherapeutic applications in human osteosarcoma.

Authors' Notes

Su Pan and Hongcun Xing contributed equally to this study.

Declaration of Conflicting Interests

The author(s) declared no potential conflicts of interest with respect to the research, authorship, and/or publication of this article.

Funding

The author(s) disclosed receipt of the following financial support for the research, authorship, and/or publication of this article: This work was supported by the National Natural Science Foundation of China (Grant no. 81301289), the Youth Research Fund Project of Jilin Province Science and Technology Development Plan (20160101221JC; 20180414060GH).

References

1. Dai X, Ma W, He X, Jha RK. Review of therapeutic strategies for osteosarcoma, chondrosarcoma, and Ewing's sarcoma. *Med Sci Monit*. 2011;17(8):RA177-RA190.
2. Boisselier E, Astruc D. Gold nanoparticles in nanomedicine: preparations, imaging, diagnostics, therapies, and toxicity. *Chem Soc Rev*. 2009;38(6):1759-1782.
3. Chen Z, Chen Z, Zhang A, Hu J, Wang X, Yang Z. Electrospun nanofibers for cancer diagnosis and therapy. *Biomater Sci*. 2016; 4(6):922-932.
4. Kang C, Sun Y, Zhu J, et al. Delivery of nanoparticles for treatment of brain tumor. *Curr Drug Metab*. 2016;17(8):745-754.
5. Xie J, Yang Z, Zhou C, Zhu J, Lee RJ, Teng L. Nanotechnology for the delivery of phytochemicals in cancer therapy. *Biotechnol Adv*. 2016;34(4):343-353.
6. Ye Z, Wei L, Zeng X, et al. Background-free imaging of a viral capsid proteins coated anisotropic nanoparticle on a living cell membrane with dark-field optical microscopy. *Anal Chem*. 2018; 90(2):1177-1185.
7. Yang Z, Yu B, Zhu J, et al. A microfluidic method to synthesize transferrin-lipid nanoparticles loaded with siRNA LOR-1284 for therapy of acute myeloid leukemia. *Nanoscale*. 2014;6(16): 9742-9751.
8. Zhou C, Yang Z, Teng L. Nanomedicine based on nucleic acids: pharmacokinetic and pharmacodynamic perspectives. *Curr Pharm Biotechnol*. 2014;15(9):829-838.
9. Farrag SM, Hamzawy MA, El-Yamany MF, Saad MA, Nassar NN. Atorvastatin in nanoparticulate formulation abates muscle and liver affliction when coalesced with coenzyme Q10 and/or vitamin E in hyperlipidemic rats. *Life Sci*. 2018;203(15): 129-140.
10. Sun W, Yang Y, Yu H, Wang L, Pan S. The synergistic effect of microwave radiation and hypergravity on rats and the intervention effect of rana sylvatica le conte oil. *Dose Response*. 2017;15(2): 1559325817711511.
11. Hongmei Y, Pan Zhaogng Yang S, Tian J, Wang L, Sun W. Hypoxic preconditioning promotes the translocation of protein kinase C ϵ binding with caveolin-3 at cell membrane not mitochondrial in rat heart. *Cell Cycle*. 2015;14(22): 3557-3565.
12. Li X, Guo S, Yang L, et al. Impact of antigens, adjuvants, and strains on sexually dimorphic antibody response to vaccines in mice. *Biologicals*. 2017;48(6):47-54.
13. Zhang X, Sun W, Wu X, et al. An oligodeoxynucleotide with CCT repeats restrains CpG ODN-Induced TLR9 trafficking. *Curr Pharm Biotechnol*. 2014;15(9):780-789.
14. Daniel MC, Astruc D. Gold nanoparticles: assembly, supramolecular chemistry, quantum-size-related properties, and applications toward biology, catalysis, and nanotechnology. *Chem Rev*. 2004;104(1):293-346.
15. Dreaden EC, Mackey MA, Huang X, Kang B, El-Sayed MA. Beating cancer in multiple ways using nanogold. *Chem Soc Rev*. 2011;40(7):3391-3404.
16. Loo C, Lowery A, Halas N, West J, Drezek R. Immunotargeted nanoshells for integrated cancer imaging and therapy. *Nano Lett*. 2005;5(4):709-711.
17. O'Neal DP, Hirsch LR, Halas NJ, Payne JD, West JL. Photothermal tumor ablation in mice using near infrared-absorbing nanoparticles. *Cancer Lett*. 2004;209(2):171-176.

18. Gao Z, Burrows ND, Valley NA, Schatz GC, Murphy CJ, Haynes CL. In solution SERS sensing using mesoporous silica-coated gold nanorods. *Analyst*. 2016;141(24):5088-5095.
19. Rath S, Halder O, Pradhani A, et al. White-light emission by phonon assisted coherent mixing of excitons in Au8-CdS hybrid nanorods. *Nanotechnology*. 2016;27(49):495706.
20. Wan M, Li X, Gao L, Fang W. Self-assembly of gold nanorods coated with phospholipids: a coarse-grained molecular dynamics study. *Nanotechnology*. 2016;27(46):465704.
21. Kim Ej, Kim EB, Lee SW, et al. An easy and sensitive sandwich assay for detection of Mycobacterium tuberculosis Ag85B antigen using quantum dots and gold nanorods. *Biosens Bioelectron*. 2017;87(18):150-156.
22. Alkilany AM, Nagaria PK, Hexel CR, Shaw TJ, Murphy CJ, Wyatt MD. Cellular uptake and cytotoxicity of gold nanorods: molecular origin of cytotoxicity and surface effects. *Small*. 2009; 5(6):701-708.
23. Ghosh P, Han G, De M, Kim CK, Rotello VM. Gold nanoparticles in delivery applications. *Adv Drug Deliv Rev*. 2008;60(11):1307-1315.
24. Prabaharan M, Grailer JJ, Pilla S, Steeber DA, Gong S. Gold nanoparticles with a monolayer of doxorubicin-conjugated amphiphilic block copolymer for tumor-targeted drug delivery. *Biomaterials*. 2009;30(30):6065-6075.
25. Ghosh PS, Kim CK, Han G, Forbes NS, Rotello VM. Efficient gene delivery vectors by tuning the surface charge density of amino acid-functionalized gold nanoparticles. *ACS Nano*. 2008;2(11):2213-2218.
26. Cheng Y, Samia CA, Meyers JD, Panagopoulos I, Fei B, Burda C. Highly efficient drug delivery with gold nanoparticle vectors for in vivo photodynamic therapy of cancer. *J Am Chem Soc*. 2008; 130(32):10643-10647.
27. Wang X, Li Y, Wang H, et al. Gold nanorod-based localized surface plasmon resonance biosensor for sensitive detection of hepatitis B virus in buffer, blood serum, and plasma. *Biosens Bioelectron*. 2010;26(2):404-410.
28. Mayer KM, Lee S, Liao H, et al. A label-free immunoassay based upon localized surface plasmon resonance of gold nanorods. *ACS Nano*. 2008;2(4):687-692.
29. Niidome T, Yamagata M, Okamoto Y, et al. Niidome. PEG-modified gold nanorods with a stealth character for in vivo applications. *J Control Release*. 2006;114(3):343-347.
30. Huang X, Neretina S, El-Sayed MA. Gold nanorods: from synthesis and properties to biological and biomedical applications. *Adv Mater*. 2009;21(48):4880-4910.
31. Kaushal A, Singh S, Kumar A, Kumar D. Nano-Au/cMWCNT-modified speB gene specific amperometric sensor for rapidly detecting streptococcus pyogenes causing rheumatic heart disease. *Indian J Microbiol*. 2017;57(1):121-124.
32. Hao K, He Y, Lu H, et al. High-sensitive surface plasmon resonance microRNA biosensor based on streptavidin functionalized gold nanorods-assisted signal amplification. *Anal Chim Acta*. 2017;954(23):114-120.
33. Keul HA, Moller M, Bockstaller MR. Structural evolution of gold nanorods during controlled secondary growth. *Langmuir*. 2007; 23(20):10307-10315.
34. Ho CJ, Balasundaram G, Driessen W, et al. Multifunctional photosensitizer-based contrast agents for photoacoustic imaging. *Sci Rep*. 2014;4(7):5342.
35. Huang JY, Park J, Wang W, Murphy CJ, Cahill DG. Ultrafast thermal analysis of surface functionalized gold nanorods in aqueous solution. *ACS Nano*. 2013;7(1):589-597.